Pressure Filtration of Flocculated Suspensions

Kerry A. Landman, Lee R. White, and Maria Eberl
Dept. of Mathematics, University of Melbourne, Parkville 3052, Victoria, Australia

From the development of a compressional rheology of a flocculated suspension, a number of separation processes have been modeled. With respect to the two-stage pressure filtration process of compact formation and then consolidation, the rheological formulation appears at first examination to be significantly at variance with the conventional engineering approach. The present model may be reconciled to the early engineering model. Moreover, the filtration parameters extracted from experiments can be related to the more fundamental rheological parameters, $r(\phi)$, the hindered settling factor, which is a function of solids volume fraction ϕ—it takes into account hydrodynamic interactions between local particles, which increase the drag forces. Useful estimates of the compact bed formation resistance and the formation time are provided as a function of applied pressure. The initial time dependence of the consolidation ratio on the elapsed consolidation time is not found to be a square root behavior as suggested by the conventional modeling.

Introduction

Over the last few years, we have developed a compressional rheology (Buscall and White, 1987) of flocculated suspension and applied this phenomenology to model a number of separation processes: batch settling (Howells et al., 1990), steady-state gravity thickening (Landman et al., 1988), and pressure filtration (Landman et al., 1991; Landman and Russel, 1993). With respect to pressure filtration, the compressional rheology formulation developed by us (Landman et al., 1991) appears at first examination to be significantly at variance with the conventional engineering approach of Wakeman et al. (1991), Shirato et al. (1986), Terzaghi (Terzaghi and Peck, 1948; Taylor, 1962), and Sivaram and Swamee (1977). The aim of the present article is to show how the present model can be reconciled to the early engineering modeling and how the filtration parameters of that modeling (extracted from filtration experiments) can be related to the more fundamental rheological parameters of our present model. To achieve this end, we must first summarize the rheological model and its assumptions.

Compressional Rheological Model

When the particles of a stable suspension are made attractive to one another, either by lowering electrostatic barriers with the addition of salt or the introduction of bridging forces with the addition of polymer, connected aggregate structures of many particles (flocs) are produced. Once the average volume fraction of these flocs is high enough, a network of connected particles throughout the suspension will form, and the suspension will assume the properties of a solid structure. Compressive stresses on the particles of the suspension are transmitted throughout the network. We need to introduce the concept of a solid stress p_s (or particle pressure) in the network and allow the concept that provided p_s is sufficiently small the network will remain solidlike and resist compression. Ultimately as the applied compressive force (such as gravity or piston pressure) is increased, a point will be reached where the network is no longer able to resist elastically and will yield and irreversibly consolidate, that is, bonds between particles will break or rearrange, more particle–particle contacts will be made, and on removal of the compressive force the network will be unable to return to its original state.

We introduce, therefore, the concept of the network possessing a compressive yield stress $P_y(\phi)$. We assume this is an implicit function of the strength of the interparticle bridging force and the previous shear history of the system during the flocculation process, and an explicit function of the local volume fraction ϕ of the solids. It is expected that $P_y(\phi)$ would increase with ϕ since the more particles per unit volume the more interconnections between particles, and consequently the stronger the networked structure (Figure 1). We also expect $P_y(\phi)$ to vanish below the volume fraction ϕ_g at

Correspondence concerning this article should be addressed to Kerry A. Landman.

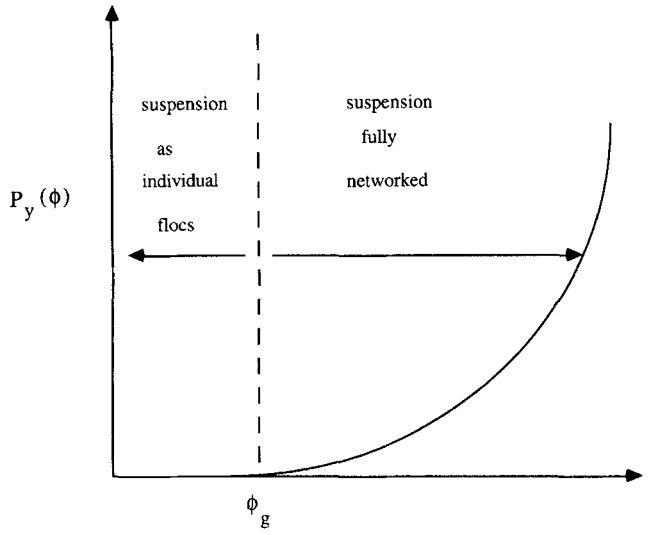

Figure 1. Form of the compressive yield stress $P_y(\phi)$ in the flocculated suspension.

which the suspension is completely networked (percolation threshold or gel point). This volume fraction would also be expected to depend on the implicit factors given earlier since the primary floc size and internal structure would be determined by these factors. We have discussed previously (Buscall and White, 1987) how the compressive yield stress $P_y(\phi)$ can be experimentally measured for any given flocculated suspension by a centrifuge technique. Power law expressions of the form

$$P_y(\phi) = k\left[\left(\frac{\phi}{\phi_g}\right)^n - 1\right] \tag{1}$$

or

$$P_y(\phi) = k\left(\frac{\phi}{\phi_g} - 1\right)^n \tag{2}$$

have been used to fit experimental $P_y(\phi)$ data, with various values of k and n. Auzerais et al. (1988) use

$$P_y(\phi) = k\left(\frac{\phi^n}{\phi_{cp} - \phi}\right) \quad \text{for} \quad \phi \gg \phi_g \tag{3}$$

where ϕ_{cp} is the close-packing volume fraction.

Armed with this rheological parameter for our flocculated suspension we can then describe the dynamic compression of the network by (Buscall and White, 1987)

$$\frac{D\phi}{Dt} = \begin{cases} 0 & p_s < P_y(\phi) \\ \kappa(\phi)[p_s - P_y(\phi)] & p_s > P_y(\phi) \end{cases} \tag{4}$$

where $D\phi/Dt$ is the material derivative of the local volume fraction, that is, the rate of change of volume fraction as we follow a particular element of the network through the separation process being modeled. The dynamic compressibility $\kappa(\phi)$ is then a second rheological parameter that appears necessary in this model. If, however, we accept the hypothesis that the hydrodynamic drainage of water from between the network structure is the rate-determining step in the consolidation process, we can estimate (Buscall and White, 1987) the magnitude of $\kappa(\phi)$. We have shown that in this picture $\kappa(\phi)$ is a very large parameter (Buscall and White, 1987; Howells et al., 1990) if once p_s exceeds $P_y(\phi)$, collapse rapidly readjusts the network local volume fraction until $P_y(\phi)$ at that volume fraction exactly matches p_s. In this large dynamic compressibility limit, we do not need the $\kappa(\phi)$ parameter and may replace Eq. 4 by

$$p_s(\mathbf{r},t) = P_y(\phi(\mathbf{r},t)) \tag{5}$$

at any point $\mathbf{r}$ and time t in the suspension. This simplifies the modeling enormously.

The equations for a one-dimensional model of pressure filtration are (Landman et al., 1991; Landman and Russel, 1993)

$$\frac{\partial p_s}{\partial z} = \frac{\lambda}{V_p}\frac{\phi r(\phi)}{1-\phi}(u-w) \tag{6}$$

where

$$\frac{\partial p_s}{\partial z} = \frac{dP_y}{d\phi}(\phi(z,t))\frac{\partial \phi}{\partial z} \tag{7}$$

for the solid phase, and

$$\frac{\partial p_f}{\partial z} = -\frac{\lambda}{V_p}\frac{\phi r(\phi)}{1-\phi}(u-w) \tag{8}$$

for the fluid phase. The spatial direction z lies normal to the filter membrane directed toward the piston (Figure 2). When

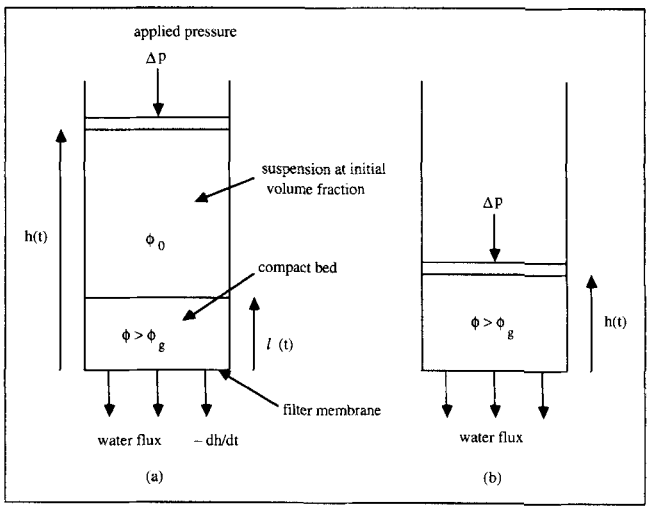

Figure 2. Two stages of filtration of an initially unnetworked ($\phi_0 < \phi_g$) suspension.

(a) Compact-bed formation; (b) consolidation of compact bed.

the gravitational sedimentation time is much longer than the filtration time as assumed here, the gravitational forces can be neglected (Landman and Russel, 1993). Physically Eq. 6 represents a force balance of the network stress gradient in the solids phase and the hydrodynamic drag on the network caused by the solid phase moving at a different velocity $-u\hat{z}$ to that of the local fluid $-w\hat{z}$. The parameter λ is a Stokes drag coefficient for an isolated solid particle ($6\pi\eta a_p$ for a spherical particle of radius a_p and fluid viscosity η). [Here there appears an "additional" factor $1-\phi$ in the denominator from the corresponding equation via Eq. 2 of Landman et al. (1991)—this comes from writing the fluid and solid equations down explicitly and rearranging those equations (Landman and Russel, 1993).]

The parameter $r(\phi)$ is a factor that accounts for the hydrodynamic interaction between local particles that increases the drag on any given particle. It might be thought of as a hindered settling factor or as a Darcy's law constant for flow in a porous media. One can seek to represent it by simple power law (references in Landman and White, 1992)

$$r(\phi) = (1 - b\phi)^m \tag{9}$$

or Kozeny-Carman-type expressions (Theis-Weesie and Phlipse, 1994), as chosen in Table 1, or empirically obtain expressions such as that of Auzerais et al. (1990). Preferably it should be regarded as another rheological parameter to be experimentally determined for the particular suspension under study. Methods for measuring $r(\phi)$ have been discussed by Landman and White (1992).

Equation 8 is the equivalent force balance for fluid motion in the suspension, where p_f is the hydrodynamic pressure in the fluid phase. These equations together with the continuity equations

$$\frac{\partial \phi}{\partial t} = \frac{\partial (\phi u)}{\partial z} \tag{10}$$

$$\frac{\partial}{\partial t}(1-\phi) = \frac{\partial}{\partial z}((1-\phi)w) \tag{11}$$

constitute the present rheological model. They may be immediately simplified. Adding Eqs. 10 and 11, we obtain

Table 1. Rheological Functions for the Flocculated Suspensions

Compressive Yield Stress ($\phi > \phi_g$)	
Data 1:	$P_y(\phi) = k(\phi^5 - \phi_g^5)$
Data 2, 3:	$P_y(\phi) = k\left(\dfrac{\phi^4 - \phi_g^4}{\phi_{cp} - \phi}\right), \quad \phi_{cp} = 0.64$
	$(\phi_g = 0.1, \quad \phi_0 = 0.05)$
Hindered Settling Factor/Permeability	
	$\dfrac{r(\phi)}{(1-\phi)^2} = \dfrac{u_{st}}{V(\phi)}$
Data 1, 2:	$V(\phi) = u_{st}(1-\phi)^{5.5}$
Data 3:	$V(\phi) = u_{st}\dfrac{(1-\phi)^3}{\phi}$

$$\frac{\partial}{\partial z}(\phi u + (1-\phi)w) = 0, \tag{12}$$

which, on integration and evaluation at the piston $z = h(t)$, where particle and fluid velocity vectors both equal $(dh/dt)\,\hat{z}$, becomes

$$\phi u + (1-\phi)w = -\frac{dh}{dt}. \tag{13}$$

This serves to elin nate the fluid velocity from the problem, since we can write

$$u - w = \frac{\left[\dfrac{dh}{dt} + u\right]}{(1-\phi)}. \tag{14}$$

Adding Eqs. 6 and 8, we obtain

$$\frac{\partial}{\partial z}(p_s + p_f) = 0, \tag{15}$$

which on integrating and evaluating at the piston yields

$$p_s(z,t) + p_f(z,t) = \Delta p \tag{16}$$

where Δp is the applied piston pressure. In general it could be some specified function of time, but in this article we shall assume it to be a given constant. The aim of the modeling is to predict $h(t)$ as a function of Δp and the rheological parameters of the theory.

We shall restrict ourselves here to the case where the initial volume fraction of the suspension ϕ_0 is less than the gel volume fraction ϕ_g so that initially the system consists of isolated (unconnected) flocs. In this case, we can identify two stages in the filtration process, as shown in Figure 2. The first stage is the formation of a compact bed that builds up on the filter membrane as individual flocs are delivered to the membrane by the fluid flux that exits through the membrane. In the compact bed the local volume fraction $\phi(z,t)$ exceeds ϕ_g and the compressive yield stress $P_y(\phi(z,t))$ is therefore nonzero. The particle stress gradient (which is z derivative of $P_y(\phi(z,t))$ is locally balanced by the hydrodynamic drag on the compact. The height of this compact bed $l(t)$ increases as filtration proceeds. The volume fraction in the compact bed is not uniform in z. This follows from the observation that $P_y(\phi)$ must be zero at the top of the bed $[z = l(t)]$ since the individual flocs above this point can transmit no particle stress.

Thus

$$\phi[l(t),t] = \phi_g. \tag{17}$$

At the filter membrane the fluid pressure $p_f(0,t)$ is effectively zero if we can neglect the hydraulic resistance of the filter membrane, since only a very small fluid pressure gradient across the membrane is needed to produce the water flux $-dh/dt$ through the filter. It follows from Eq. 16 that

$$p_s(0,t) = P_y[\phi(0,t)] = \Delta p, \tag{18}$$

so that $\phi(0,t)$ is immediately fixed (independent of time) as the solution of Eq. 18 once $P_y(\phi)$ is determined for the suspension under study. Clearly $\phi(0) > \phi_g$. Thus we have established that the volume fraction in the compact bed varies from $\phi(0)(>\phi_g)$ at the membrane to ϕ_g at the top of the bed. Therefore the hydrodynamic resistance of the compact bed is not a constant throughout the bed, since it depends on the local volume fraction as $(\lambda/\eta V_p)[\phi r(\phi)/(1-\phi)]$ (through Eq. 6). We will return to this point below.

Above the compact bed, the suspension exists as individual flocs transported toward the membrane and the top of the compact bed by the fluid flow moving with the fluid

$$u(z,t) = w(z,t) = -\frac{dh}{dt}. \tag{19}$$

The volume fraction in $l(t) < z < h(t)$ remains at the initial value $\phi_0(<\phi_g)$ so that

$$p_s(z,t) = P_y(\phi_0) = 0, \tag{20}$$

and hence

$$p_f(z,t) = \Delta p \tag{21}$$

in this region. We illustrate the time evolution of the compact bed stage in the filtration process in Figure 3.

At time $t = t_f$ the compact bed height $l(t_f)$ reaches the piston $h(t_f)$. From this point there is no unnetworked suspension at ϕ_0 between the piston and the membrane, and we enter the second filtration stage, consolidation of the compact bed. Since we continue to require $p_f(0,t)$ to be negligible, during this stage the volume fraction at the membrane remains at the original fixed number $\phi(0)$ obtained from solving Eq. 18. At the end of filtration, we will obtain a uniform bed at this volume fraction since at equilibrium there will be zero fluid pressure in the bed and the solids stress must (from Eq. 16) be equal to the applied pressure Δp throughout the cake. The final bed height at equilibrium is then

$$h_\infty = \frac{h_0\phi_0}{\phi(0)}. \tag{22}$$

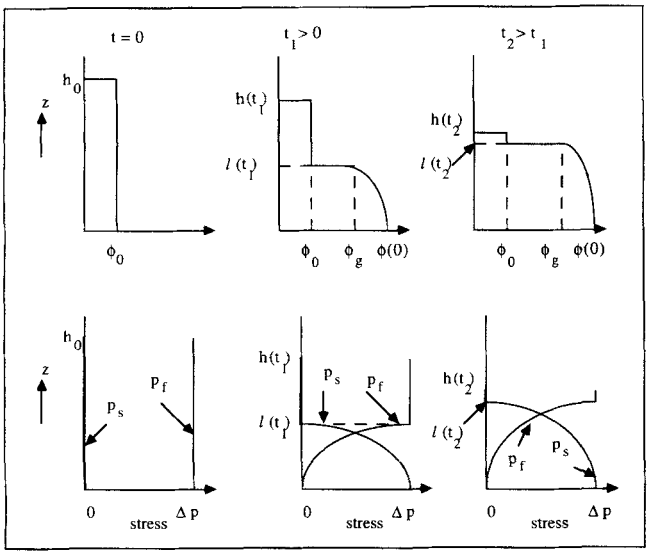

Figure 3. Physical picture of the compact-bed formation stage.

The detailed computation of this model has been described by us elsewhere (Landman et al., 1991) and will not be repeated here. We are concerned here with making the connection between this model and the conventional engineering model of Shirato et al. (1986) and Wakeman et al. (1991) for compact formation and that of Terzaghi (Terzaghi and Peck, 1948; Taylor, 1962) for the consolidation stage.

Compact Formation Modeling

In the Shirato-Wakeman model of the compact bed formation state, the total pressure drop in the fluid phase (which must equal the applied piston pressure Δp) is considered to be the sum of a pressure drop across the growing compact bed and a pressure drop across the membrane

$$\Delta p = \eta\alpha c V\frac{dV}{dt} + \eta R\frac{dV}{dt} \tag{23}$$

or

$$\frac{dV}{dt} = \frac{\Delta p}{\eta\alpha c V + \eta R}. \tag{24}$$

Here $V(t)$ is the volume of fluid expressed per unit area of membrane. Thus

$$V(t) = h_0 - h(t) \tag{25}$$

and the water flux is then

$$\frac{dV}{dt} = -\frac{dh}{dt}, \tag{26}$$

R is a membrane hydraulic resistance, and c is the effective solids mass concentration in the filter feed [so that $cV(t)$ is the mass of the compact bed at time t]. The quantity α in this theory is the compact bed hydraulic resistance per unit mass of bed and is assumed constant as the bed grows. In the rheological model presented earlier, this assumption would be clearly invalid since the hydrodynamic drag exerted by the particles on the fluid would be a strong function of volume fraction that we have shown varies from the final solids volume fraction at the membrane to the gel volume fraction at the top of the compact bed.

Integrating Eq. 24, assuming a constant Δp, and keeping α fixed leads to

$$\frac{t}{V} = \left(\frac{\alpha c\eta}{2\Delta p}\right)V + \left(\frac{\eta R}{\Delta p}\right), \tag{27}$$

which predicts that a plot of t/V vs. V should yield a straight line in the compact formation stage ($t < t_f$), whose slope yields

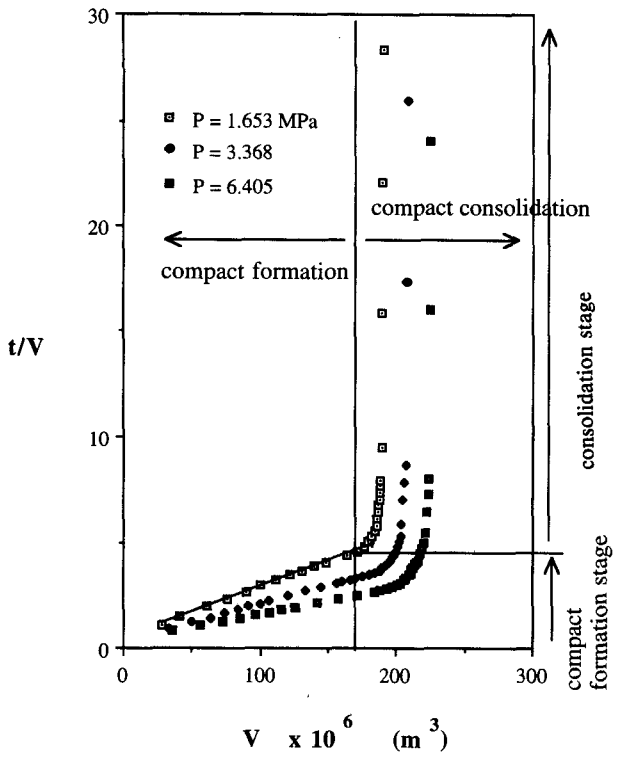

Figure 4. *t/V* vs. *V* data replotted from Wakeman et al. (1991) for hydromagnesite for various applied pressures.

The graph for $\Delta p = 1.653$ MPa has been annotated for the two stages.

the resistance per unit mass α of the compact and the intercept yields the membrane resistance. Wakeman et al. (1991) exhibit such curves for hydromagnesite and china clay. In Figure 4 we replot some of this hydromagnesite filtration data (obtained through Wakeman). Clearly the experimental data obeys Eq. 27, and this method of plotting filtration data dramatically exhibits the two-stage nature of the filtration process. There are considerable variations in the compact formation time t_f and consolidation time t_c from hydromagnesite to china clay and considerable variation in α as a function Δp. The inherent weakness in this sort of modeling (its ability to summarize data notwithstanding) is that no insight is gained into why t_c, t_f, and α behave in the observed way with the control parameters. There is little predictive power in this modeling exercise—to design an industrial filtration process or understand its malfunction one reproduces in the laboratory the process itself. The rheological model for all its greater level of complexity does reduce the process to a set of measurable rheological parameters that control the process. We now discuss how the two approaches can be reconciled.

We proceed by making some simplifying assumptions in the rheological model developed in the previous section. First we neglect the solids velocity $u(z,t)$ in comparison with dh/dt in the compact bed zone $0 < z < l(t)$. We will show below that this is an excellent approximation. It is certainly true that

$$u(0,t) = 0 \tag{28}$$

since solids cannot pass the membrane. However, the conservation of solids equation

$$\int_0^{l(t)} \phi(z,t)dz + \phi_o[h(t) - l(t)] = \phi_0 h_0 \tag{29}$$

may be differentiated with respect to t to reveal (using Eq. 10)

$$u(l,t) = \left(\frac{\phi_0}{\phi_g}\right)\frac{dh}{dt} + \left(1 - \frac{\phi_0}{\phi_g}\right)\frac{dl}{dt}, \tag{30}$$

which implies u at the top of the bed is of the order of dh/dt. The validity of the approximation lies in the fact that dl/dt is positive and dh/dt is negative, and therefore $u(l,t)$ is substantially smaller than $-d_h/dt$. Using Eq. 14, the fluid force balance equation (Eq. 8) can be written as

$$\frac{\partial p_f}{\partial z} = -\frac{\lambda}{V_p}\frac{\phi r(\phi)}{(1-\phi)^2}\left(\frac{dh}{dt} + u\right). \tag{31}$$

Neglecting u in comparison to dh/dt and integrating this equation across the compact bed, we obtain

$$\Delta p = p_f(l(t),t) = p_f(0,t) - \frac{\lambda}{V_p}\left\{\int_0^{l(t)} \frac{\phi r(\phi)dz}{(1-\phi)^2}\right\}\frac{dh}{dt}, \tag{32}$$

but

$$p_f(0,t) = -\eta R\frac{dh}{dt} \tag{33}$$

assuming Darcy's law flow through the filter membrane. Thus we can write

$$\frac{dV}{d} = -\frac{dh}{dt} = \frac{\Delta p}{\frac{\lambda}{V_p}\left\{\int_0^{l(t)} \frac{\phi r(\phi)}{(1-\phi)^2}dz\right\} + \eta R}. \tag{34}$$

From Eqs. 29 and 25 we have that

$$V(t) = \int_0^{l(t)}\left(\frac{\phi(z,t)}{\phi_0} - 1\right)dz. \tag{35}$$

We can therefore write the rheological model in this approximation as

$$\frac{dV}{dt} = \frac{\Delta p}{\frac{\lambda}{V_p}\left\{\frac{\int_0^{l(t)} \frac{\phi r(\phi)}{(1-\phi)^2}dz}{\int_0^{l(t)}\left(\frac{\phi}{\phi_0} - 1\right)dz}\right\}V + \eta R} \tag{36}$$

and thus observe that the Shirato-Wakeman approach (Eq. 24) may be reconciled with this approximate rheological

model (Eq. 36) provided that the ratio of integrals in brackets in the denominator of Eq. 36 is a constant with respect to time. We confirm this result below—this allows the bed resistance per unit mass parameter to be identified with rheological model functions as

$$\alpha c = \frac{\lambda}{\eta V_p} \frac{\int_0^{l(t)} \frac{\phi r(\phi)}{(1-\phi)^2} dz}{\int_0^{l(t)} \left(\frac{\phi}{\phi_0} - 1 \right) dz}. \tag{37}$$

In Appendix 1, when the membrane resistance is negligible, we demonstrate that a similarity solution of the exact rheological model equation exists in the form

$$\phi(z,t) = \phi_0 \Phi(\xi) \tag{38}$$

where ξ is the similarity variable

$$\xi = \frac{Z}{\sqrt{T}} \tag{39}$$

and where Z, T are scaled z, t variables. The heights are found as

$$\frac{h(t)}{h_0} = 1 - \beta\sqrt{T} \tag{40}$$

$$\frac{l(t)}{h_0} = \gamma\sqrt{T}. \tag{41}$$

The numerical constants β and γ are determined simultaneously with the function $\Phi(\xi)$ as the solution of a second-order nonlinear ordinary differential equation with appropriate boundary conditions, as discussed in Appendix 1.

It follows immediately that

$$\frac{V(t)}{h_0} = \beta\sqrt{T} \tag{42}$$

and therefore that

$$\frac{T}{V} = \frac{\sqrt{T}}{h_0 \beta} = \left\{ \frac{1}{h_0^2 \beta^2} \right\} V. \tag{43}$$

The exact (no approximations) rheological model therefore predicts that t/V is linear in V, and in unscaled variables predicts that

$$\text{slope (exact)} = \frac{1}{\beta^2} \left[\frac{\lambda}{V_p} \frac{\phi_0 r(\phi_0)}{k(1-\phi_0)^2} \right] \tag{44}$$

where k is the chosen suitable scale for pressure in the system (see Eqs. 1–3 or Table 1). The pressure scale can be chosen to be any convenient value of $P_y(\phi)$; for example, in Landman et al. (1991), it was chosen as $P_y(\phi_0 + \phi_g)$. The dependence of β and γ on $\Delta p/k$ for three different systems in Table 1 is shown in Figure 5.

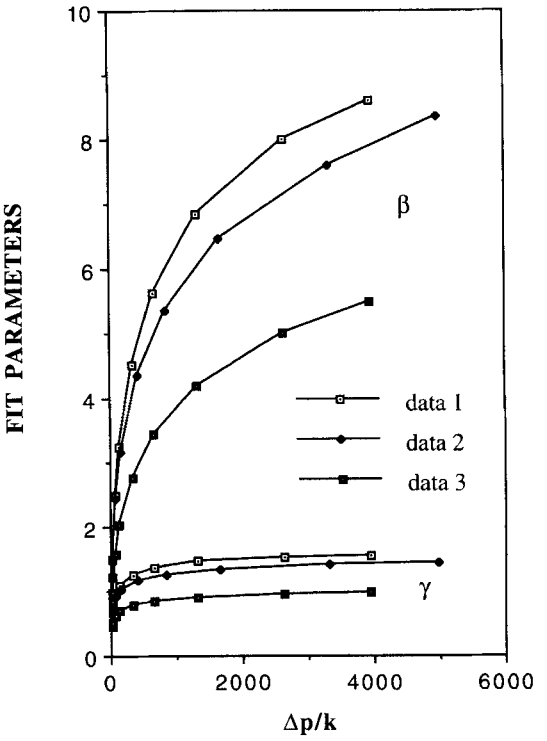

Figure 5. Dependence of β and γ on $\Delta p/k$ for the three systems in Table 1.

Consequently the dependence of the slope of the t/V vs. V plot on piston pressure is directly predictable from the rheological model and is not restricted to empirical determination.

It also follows that in the approximate rheological model (neglect of particle velocity in the compact bed) the ratio of time-dependent integrals is independent of time since

$$\frac{\int_0^{l(t)} \frac{\phi r(\phi)}{(1-\phi)^2} dz}{\int_0^{l(t)} \left(\frac{\phi}{\phi_0} - 1 \right) dz} = \frac{\phi_o r(\phi_0)}{(1-\phi_0)^2} \frac{\int_0^{\gamma} \Phi(\xi) R[\Phi(\xi)] d\xi}{\int_0^{\gamma} \Phi(\xi) d\xi} \tag{45}$$

where

$$R(\Phi) = \frac{r(\phi)(1-\phi_0)^2}{(1-\phi)^2 r(\phi_0)} \tag{46}$$

by changing the integration variable from z to the similarity variable ξ.

We are now in a position to test the approximation that $u(z,t)$ can be neglected in comparison with dh/dt in the compact bed. The slope of t/V vs. V in the approximate theory is (from Eqs. 37 and 45)

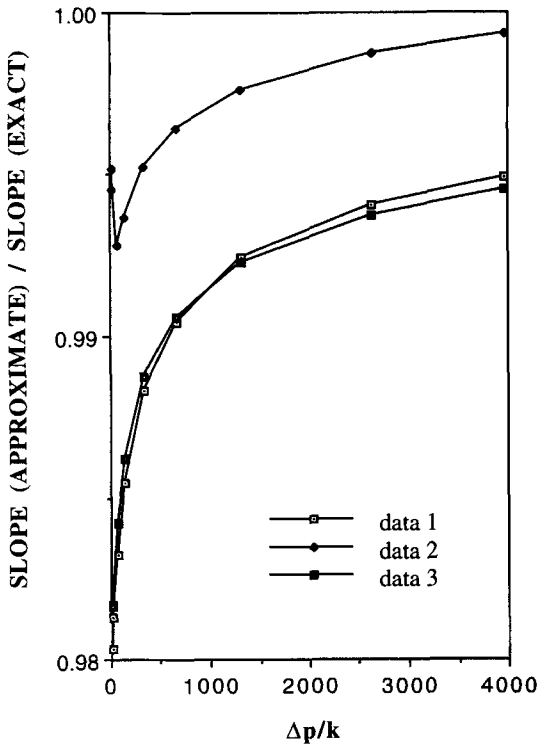

Figure 6. Ratio of the approximate slope of t/V vs. V over the exact slope for the three data sets in Table 1.

Values near unity indicate the validity of the approximation $u(z, t)$ is negligible compared to dh/dt in the compact bed.

$$\text{slope (approx)} = \frac{1}{2\Delta p}\left(\frac{\lambda}{V_p}\right)\frac{\phi_0 r(\phi_0)}{(1-\phi_0)^2}\frac{\int_0^{\gamma}\Phi R(\Phi)d\xi}{\int_0^{\gamma}(\Phi-1)d\xi}. \quad (47)$$

It follows that if we can neglect $u(z,t)$ in the compact bed, then

$$\frac{\text{slope (approx)}}{\text{slope (exact)}} = \frac{\beta^2}{2(\Delta p/k)}\frac{\int_0^{\gamma}\Phi R(\Phi)d\xi}{\int_0^{\gamma}(\Phi-1)d\xi} \quad (48)$$

should be ~ 1. In Figure 6 we plot this ratio as a function of $(\Delta p/k)$ over a wide range of pressure valves for three different systems as described in Table 1. For all cases examined the approximation is valid to a few percent. This agreement between approximate and exact numerical calculation is useful since it serves to provide a direct estimate of the compact resistance factor α and its piston pressure dependence.

The mean value theorem enables us to write

$$\int_0^{l(t)}\frac{\phi r(\phi)}{(1-\phi)^2}dz = \frac{\phi_1 r(\phi_1)}{(1-\phi_1)^2}l(t) \quad (49)$$

where $\phi_g < \phi_1 < \phi(0)$. Similarly we can write

$$\int_0^{l(t)}\left(\frac{\phi}{\phi_0}-1\right)dz = \left(\frac{\phi_2}{\phi_0}-1\right)l(t) \quad (50)$$

where, again, $\phi_g < \phi_2 < \phi(0)$. Now, in general, we can categorically assert that $\phi_1 \neq \phi_2$. If, however, we argue that approximately,

$$\phi_1 = \phi_2 = \phi_m, \quad (51)$$

then we have (from Eq. 37)

$$\alpha c = \frac{\lambda}{\eta V_p}\frac{\phi_m r(\phi_m)}{(1-\phi_m)^2\left(\frac{\phi_m}{\phi_0}-1\right)}. \quad (52)$$

If Eq. 51 were roughly correct, then we have in Eq. 52 a ready estimate of the slope of the t/V vs. V plot for compact bed formation. This would be useful if we can find a rule for determining ϕ_m, which would hold for all piston pressure values of likely interest.

In Figure 7 we show the accuracy of Eq. 52 for the Table 1 systems using various choices for ϕ_m by plotting the ratio of the slope according to the mean value approximation (Eq. 52) to the exact slope. The volume fraction within the bed is nonuniform and varies between $\phi(0)$ and ϕ_g in a nonlinear way. Various choices of ϕ_m were tried, for example, the membrane volume fraction

$$\phi_m = \phi(0), \quad (53)$$

the mean bed volume fraction

$$\phi_m = \frac{1}{l(t)}\int_0^{l(t)}\phi dz, \quad (54)$$

the average bed volume fraction

$$\phi_m = \frac{1}{2}[\phi(0)+\phi_g], \quad (55)$$

and a combined average and membrane volume fraction, namely

$$\phi_m = \frac{1}{2}[\text{average}+\phi(0)] = \frac{3}{4}\phi(0)+\frac{1}{4}\phi_g. \quad (56)$$

We observed that the choice (Eq. 56) made the ratios close to unity over a wide range of applied pressures Δp. The agreement is not perfect, but in order to understand the pressure dependence of the slope, Eq. 52 is remarkably instructive. Recall that to determine $\phi(0)$ the volume fraction at the membrane as a function of Δp, we solve Eq. 18 for a given Δp. We then compute ϕ_m via Eq. 56, and knowledge of $r(\phi)$ enables us to predict the slope with considerable precision from the mean value approximate expression (Eq. 52).

Since we have used only a few data sets to produce this empirical observation, it is by no means proved, but the agreement over such a large applied pressure range is im-

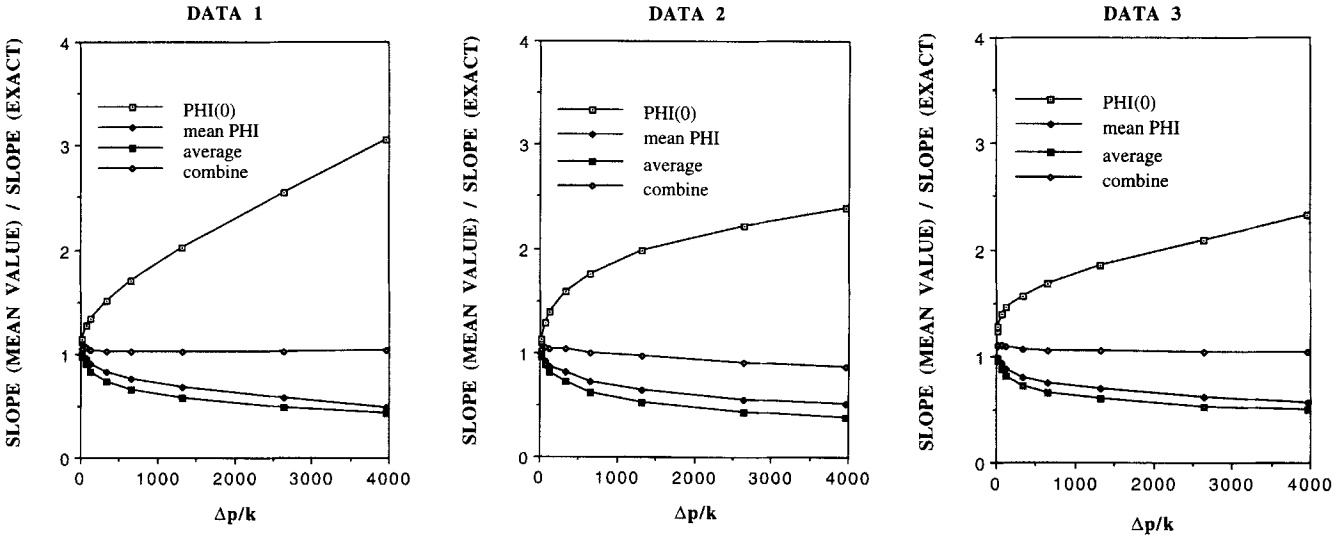

Figure 7. Ratio of the t/V vs. V slope for the mean value approximation (Eq. 52) and exact slope for the three data sets in Table 1 for various choices of ϕ_m.

PHI(0) = $\phi(0)$; mean PHI = $1/l(t)\int_0^{l(t)}\phi\,dz$; average = $1/2\,(\phi(0)+\phi_g)$; combine $3/4\,\phi(0)+1/4\,\phi_g$.

pressive. Interestingly, none of the choices (Eqs. 53–55) are as good as Eq. 56 in predicting the slope via Eq. 52.

The time t_f to the end of compact formation when $l(t_f) = h(t_f)$ is given exactly in the rheological model by (from Eqs. 40 and 41)

$$t_f(\text{exact}) = \frac{\lambda}{V_p}\frac{\phi_0 r(\phi_0)h_0^2}{k(1-\phi_0)^2}\left\{\frac{1}{(\beta+\gamma)^2}\right\} \tag{57}$$

and the piston height at this time is

$$h(t_f) = \left(\frac{\gamma}{\gamma+\beta}\right)h_0. \tag{58}$$

We may also examine a mean value approximation to estimate t_f. The conservation equation (Eq. 29) can be written as

$$\phi_2 l + \phi_0(h-l) = \phi_0 h_0 \tag{59}$$

using the mean value theorem. It follows that

$$h(t_f) = l(t_f) = \frac{\phi_0 h_0}{\phi_2}. \tag{60}$$

Again, using the approximation (Eq. 51), and a rearrangement of Eq. 27, viz.,

$$t = \frac{\alpha c\eta}{2\Delta p}(h_0-h)^2 + \frac{\eta R}{\Delta p}(h_0-h), \tag{61}$$

we can derive the mean value approximation

$$t_f(\text{approx}) \approx \frac{1}{2}\left(\frac{\lambda}{V_p}\right)\frac{\phi_0(\phi_m-\phi_0)r(\phi_m)h_0^2}{\Delta p\phi_m(1-\phi_m)^2} + \frac{\eta h_0 R(\phi_m-\phi_0)}{\Delta p\phi_m} \tag{62}$$

with the aid of Eqs. 52 and 60. This is a useful estimate of compact bed formation time, provided a rule for determining ϕ_m can be found for all Δp values of interest. In Figure 8 we show the accuracy of Eq. 62 for the three systems in Table 1 using various choices for ϕ_m by plotting the ratio of the mean value approximation (Eq. 62) to t_f and the exact t_f value (Eq. 57), for the case with $R = 0$. Again we observe that Eq. 56 is a surprisingly accurate rule for choosing ϕ_m over a wide Δp range for all the chosen data sets.

Finally, we note that the size of the individual particles enters the slope equations (such as Eq. 44) and the compact formation time equations (such as Eq. 57) only through the parameter $(\lambda/V_p) \sim (1/a_p^2)$ where a_p is a typical particle size. It is, however, difficult to verify this observation of the rheological model since it is not easy to keep the network structure [and hence $P_y(\phi)$] constant as the experimentalist changes the particle size of the suspension. Some data of Wakeman et al. (1991) on different sizes of china clay under pressure filtration show that the measured compact resistance α is such that

$$\frac{\alpha(1.3\mu)}{\alpha(5.4\mu)} \sim 24-32 \tag{63}$$

over a wide Δp range for 1.3 μ- and 5.4 μ-sized clay suspensions. The present theory would predict a ratio of 17.3, all other parameters being equal. Such an agreement is encouraging in view of the vagaries of such an experimental system.

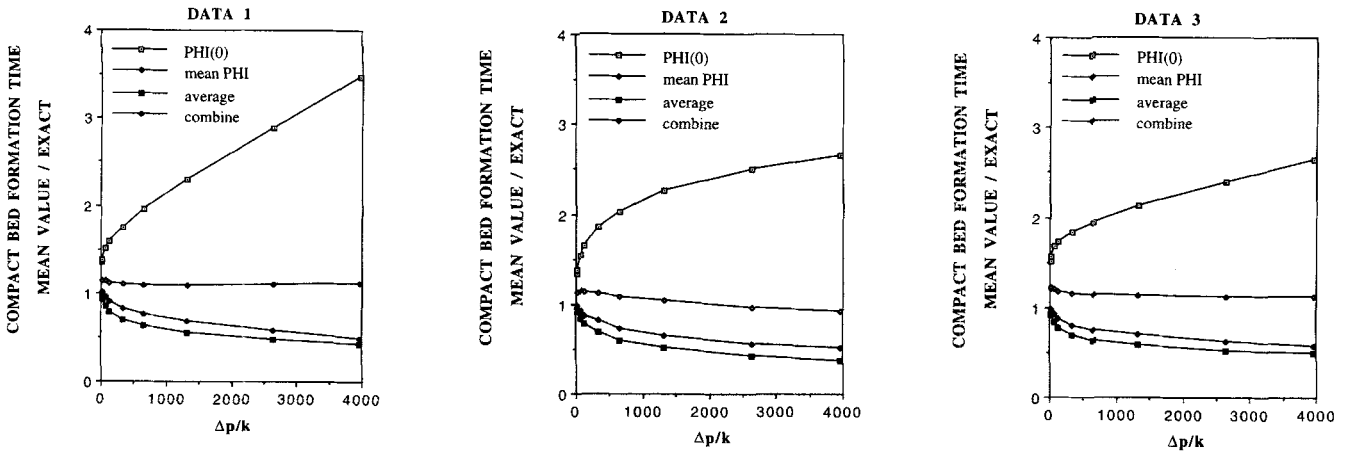

Figure 8. Ratio of the compact-bed formation time t_f for the mean value approximation (Eq. 62) and exact value (Eq. 57) for the three data sets in Table 1 for various choices of ϕ_m.

PHI(0) = $\phi(0)$; mean PHI = $1/l(t)\int_0^{h(t)}\phi\,dz$; average = 1/2 ($\phi(0)+\phi_g$); combine 3/4 $\phi(0)+1/4\,\phi_g$.

We note in addition that the slope is independent of the initial height of the suspension h_0 in the filter press and the compact formation time is proportional to h_0^2 in the rheological model. These dependencies should be easier to test experimentally, but do not distinguish the two models considered here.

Consolidation Modeling

The rheological model of the final consolidation phase of pressure filtration would require that

$$p_f(0,t) \backsim 0, \tag{64}$$

given that membrane resistance is negligible as discussed previously, and hence (from Eq. 16)

$$p_s(0,t) = P_y[\phi(0,t)] = \Delta p, \tag{65}$$

as in the compact formation stage. Since there is no longer an uncompacted region of volume fraction ϕ_0 above the compact bed, the pressure boundary conditions at the piston are now different. One can no longer assert that the solids pressure is zero at the piston; now Δp is shared between the fluid and solid phases at $z = h(t)$. Instead we now use the boundary condition

$$u[h(t),t] = -\frac{dh}{dt}, \tag{66}$$

which from Eq. A1 implies that

$$\frac{\partial\phi}{\partial z}[h(t),t] = 0. \tag{67}$$

The physical picture of the consolidation phase as it evolves in time is shown schematically in Figure 9.

Consolidation modeling has made use of the Terzaghi model (Terzaghi and Peck, 1948; Taylor, 1962) for consolidation in the soil science literature. Sivaram and Swamee (1977) developed an analytic expression that approximates the numerical solution of the Terzaghi model accurately, and as modified by Shirato et al. (1986) is

$$U_c = \frac{T_c^{1/2}}{[1+(T_c)^{\nu}]^{1/2\nu}} \tag{68}$$

where the consolidation ratio U_c is given by

$$U_c(t) = \frac{h(t_f) - h(t)}{h(t_f) - h_\infty} \tag{69}$$

and T_c is a dimensionless time variable defined by

$$T_c = \frac{4i^2 C_e (t - t_f)}{\pi(\phi_0 h_0)^2}. \tag{70}$$

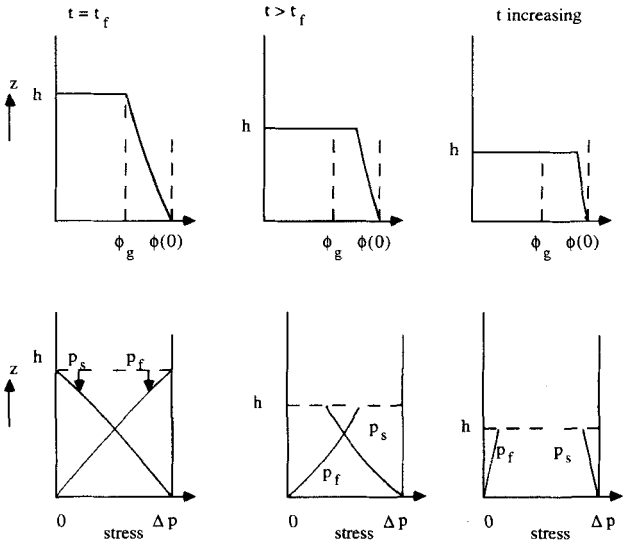

Figure 9. Physical picture of the consolidation stage.

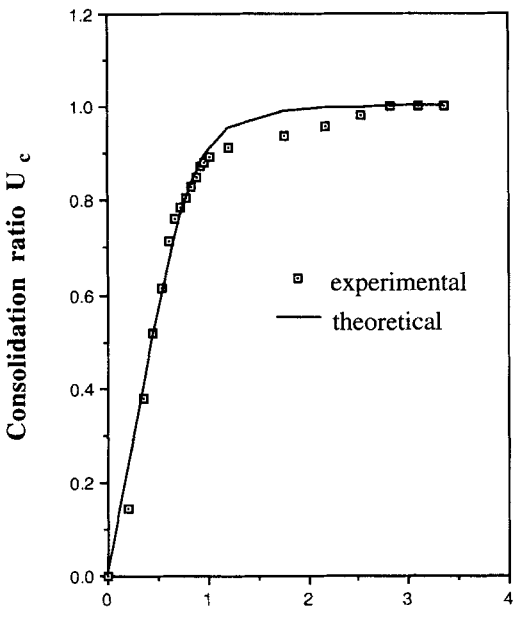

Figure 10. Consolidation ratio for hydromagnesite data in Figure 4 $\Delta p = 1.653$ MPa compared to empirical equation (Eq. 68) with $v = 2.2$ (provided by Wakeman).

Here i is the number of drainage surfaces, and C_e is a modified consolidation coefficient.

Again, this engineering theory proves very successful in summarizing the consolidation phase filtration data. As an example, we show in Figure 10 the consolidation ratio for one of the hydromagnesite data curves in Figure 4 (provided by Wakeman). It is clear that $T_c \backsim 1$ is a good measure of consolidation time t_c so that

$$t_c \approx \frac{\pi(\phi_0 h_0)^2}{4i^2 C_e}. \tag{71}$$

The consolidation time is determined experimentally as the inverse of the square of the slope of a plot of U_c against $\sqrt{t - t_f}$ for small $t - t_f$. Little insight is gained in this model as to how C_e will vary with Δp and particle size.

The rheological model also gives some insight into the bed consolidation stage. First we observe that the partial differential equation (Eq. A37) is a diffusion equation where the diffusion coefficient is given by the scaled function $D(\Phi)$ (Eq. A19). It follows directly that the consolidation time should scale as $h_\infty^2/D(\Phi)$.

Numerical solution of Eq. A37 reveals some interesting features. In Figure 11 we plot the t/V vs. V graph for two of the systems displayed in Table 1. On those plots we can exactly identify the start of the consolidation stage and have marked its position with a vertical bar. It is clear that the onset of this stage is not marked by any abrupt change in the form of the curve. If this situation translates to the experimental t/V vs. V plots, conventional modeling cannot identify the precise point at which to begin to measure consolidation time, and plots of the type shown in Figure 10 require an interactive refinement of the estimate of starting point in order to achieve the fit illustrated.

Indeed, numerical calculations on the two data sets shown

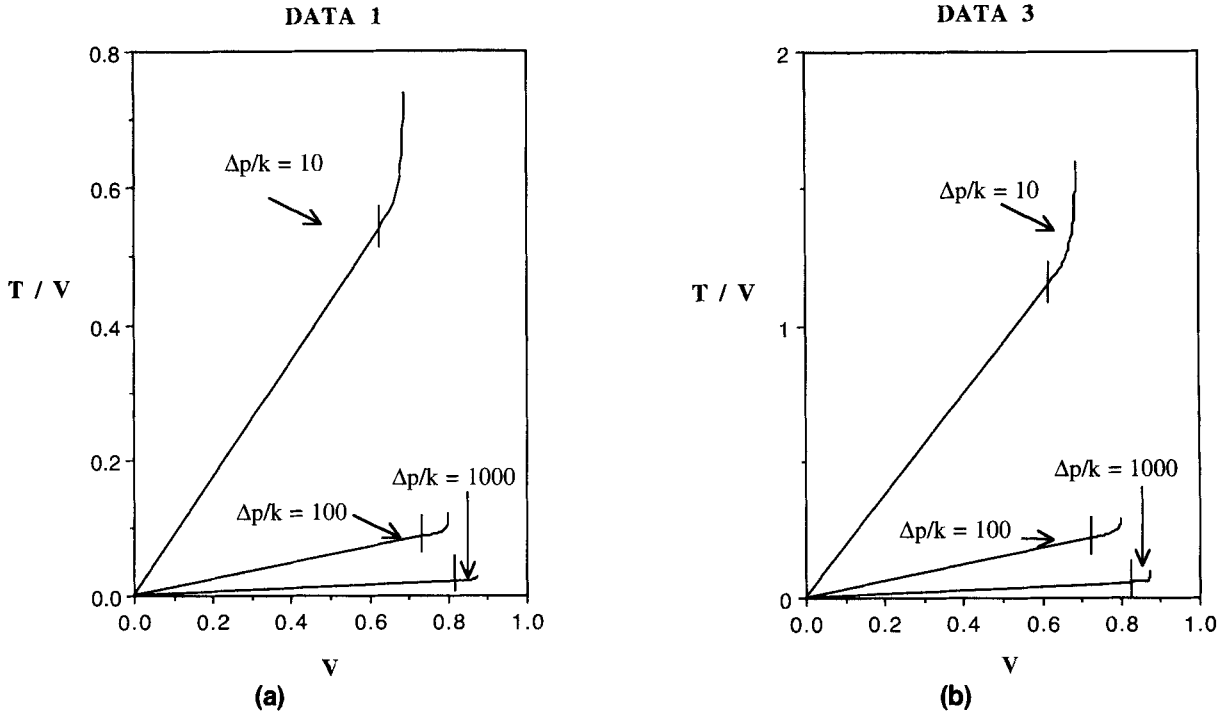

Figure 11. Numerical solution of the rheological model giving t/V vs. V for two data sets in Table 1 and several values of $\Delta p/k$.

Vertical bars mark the start of the consolidation region. (a) DATA 1. (b) DATA 3.

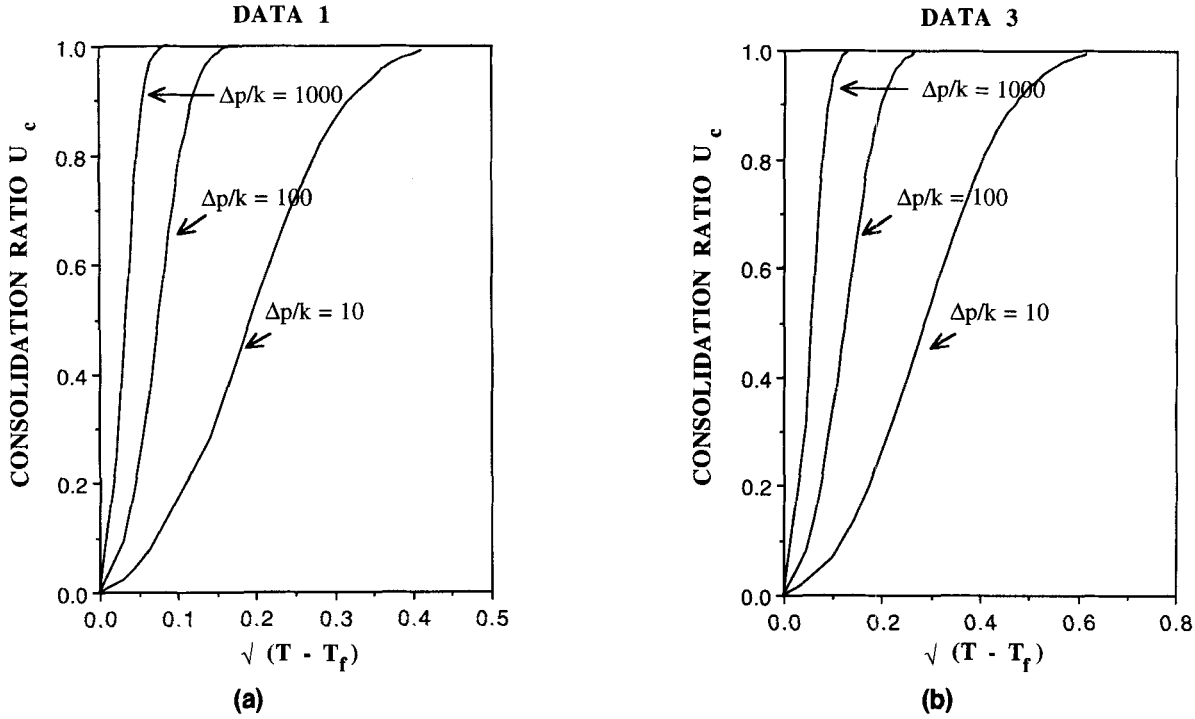

Figure 12. Consolidation ratio U_c as a function of the square root of the scaled elapsed consolidation time T-T_f for several values of $\Delta p/k$.

Vertical bars mark the start of the consolidation region. (a) DATA 1. (b) DATA 3.

in Figure 11 reveal that the initial time dependence of the consolidation ratio on elapsed consolidation time $t - t_f$ is not a square root behavior as suggested by the conventional model. This is illustrated in Figure 11 where U_c is plotted as a function of $(t - t_f)^{1/2}$ for various values of the applied pressure. This numerical study does reveal that there is a considerable linear region in such a plot and suggests that an analytic approximation can be obtained. We develop an approximate similarity solution in Appendix 2. There we show that

$$U_c = S\sqrt{t - t_f} \tag{72}$$

where

$$S = \frac{\delta}{H_f - H_\infty}\left[\frac{k(1-\phi_0)^2}{\phi_0 r(\phi_0) h_0^2}\left(\frac{V_p}{\lambda}\right)\right]^{1/2} \tag{73}$$

is valid for small $t - t_f$. Here $H_f = h(t_f)/h_0$ and $H_\infty = h_\infty/h_0$. The numerical parameter δ may be explicitly determined as discussed in Appendix 2. The dependence of δ on $\Delta p/k$ for the three different systems in Table 1 is shown in Figure 13.

For the data displayed in Figure 12a for Data 1 of Table 1 we observe a slope of $S = 7.6$ compared to the similarity model calculation of $S = 9.1$ for scaled pressure of $\Delta p/k = 100$. For $\Delta p/k = 1{,}000$ we observe $S = 17.0$ compared to the similarity model of $S = 20.6$. Such agreement is encouraging but hardly spectacular.

It is clear that more theoretical work is required in the modeling of this stage of the filtration process. Unsatisfactory features of both the conventional engineering model and the rheological model exist, and a full reconciliation of the two approaches is yet to be achieved. If we assume that Eq. 72 holds until $U_c = 1$, then we predict from the similarity model a consolidation time of S^{-2} or

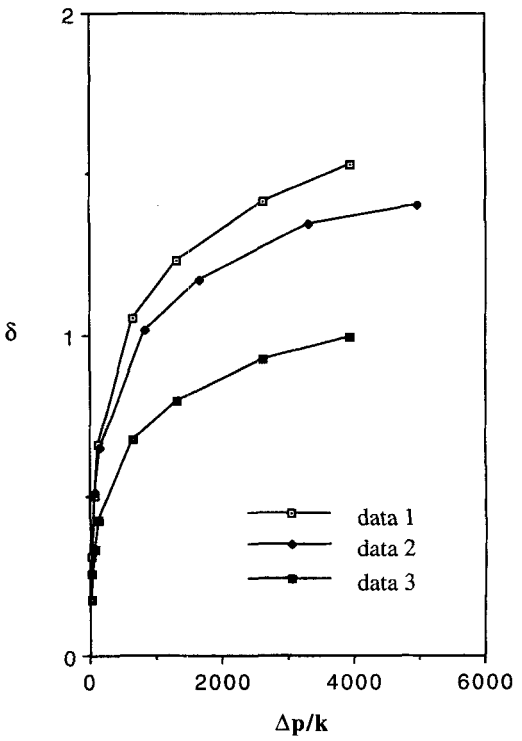

Figure 13. Dependence of δ on $\Delta p/k$ for the three systems in Table 1.

$$t_c \approx \frac{(H_f - H_\infty)^2}{\delta^2}\left[\frac{\phi_0 r(\phi_0) h_0^2}{k(1-\phi_0)^2}\left(\frac{\lambda}{V_p}\right)\right], \qquad (74)$$

and we can identify the parameter i^2C_e of the conventional model as

$$i^2C_e = \frac{\pi}{4}\left(\frac{V_p}{\lambda}\right)\frac{k\phi_0(1-\phi_0)^2\delta^2}{r(\phi_0)(H_f - H_\infty)^2}. \qquad (75)$$

However, this identification is not as physically clear as in the case of the compact resistance α, since we do not have an approximate way of writing δ as a function of the rheological parameters as we could for β in the compact formation theory.

Conclusions

In the conventional engineering approach the compact-bed formation stage in pressure filtration of a dilute suspension can be well described by a bed resistance per unit mass parameter α, which is measured from the slope of a plot of t/V vs. V. The dependence of α on applied piston pressure, particle size, and initial feed concentration can be studied experimentally. Clearly α is related in some way to the hydrodynamic drag exerted by the suspension particles on the filtrate flowing past. The rheological model can explain the value of α in terms of $r(\phi)$, the true hydrodynamic resistance parameter, or the inverse of the permeability. The pressure dependence has its origin in the volume fraction of the compact bed at the filter membrane, which in turn is connected to the applied pressure, through the mechanical requirement that the compressive yield stress at this point be equal to the applied pressure.

The second stage of pressure filtration has not yet been completely understood. We can model its dynamics numerically but do not yet possess the complete physical understanding of the role of the rheological parameters as we do in the compact formation stage. We are continuing to develop an approximate rheological model to provide physical insight and the identification of the engineering parameter i^2C_e of conventional modeling with rheological parameters.

This work reconciles the conventional engineering treatment of solid/liquid separation processes with the more physical compressional rheology model and reinterprets the engineering parameters in terms of the rheological parameters. The engineering approach (its ability to summarize data notwithstanding) gives little insight into why the separation performance behaves with control parameters in the observed manner and little predictive power. The rheological model reduces the process to a set of rheological parameters that fundamentally control the process.

Acknowledgment

This work was carried out with the support of the Australian Research Council and the International Fine Particle Research Institute, Inc.

Notation

H_∞ = scaled equilibrium bed height
n = index in yield stress function
S = constant in consolidation ratio U_c
u_0 = Stokes settling velocity of an isolated particle
$V(\phi)$ = mean settling velocity
V_p = average particle volume
β = constant in similarity solution for compact bed stage
δ = constant in similarity solution for consolidation stage
γ = constant in similarity solution for compact bed stage
ϕ = volume fraction of suspension occupied by solids

Literature Cited

Auzerais, F. M., R. Jackson, and W. B. Russel, "The Resolution of Shocks and the Effects of Compressible Sediments in Transient Settling," *J. Fluid Mech.*, **195**, 437 (1988).

Auzerais, F. M., R. Jackson, W. B. Russel, and W. F. Murphy, "The Transient Settling of Stable and Flocculated Dispersions," *J. Fluid Mech.*, **221**, 613 (1990).

Buscall, R., and L. R. White, "On the Consolidation of Concentrated Suspensions I: The Theory of Sedimentation," *J. Chem. Soc. Faraday Trans. 1*, **83**, 873 (1987).

Howells, I., K. A. Landman, A. Panjkov, C. Sirakoff, and L. R. White, "Time-dependent Batch Settling of Flocculated Suspensions," *Appl. Math Modelling*, **14**, 77 (1990).

Landman, K. A., L. R. White, and R. Buscall, "The Continuous-Flow Gravity Thickener: Steady State Behavior," *AIChE J.*, **34**, 239 (1988).

Landman, K. A., C. Sirakoff, and L. R. White, "Dewatering of Flocculated Suspensions by Pressure Filtration," *Phys. Fluids A*, **3**, 1495 (1991).

Landman, K. A., and L. R. White, "Determination of the Hindered Settling Factor for Flocculated Suspensions," *AIChE J.*, **38**, 184 (1992).

Landman, K. A., and W. B. Russel, "Filtration at Large Pressures for Strongly Flocculated Suspensions," *Phys. Fluids A*, **5**, 550 (1993).

Shirato, M., T. Murase, and M. Iwata, in *Progress in Filtration and Separation: 4*, R. J. Wakeman, ed., Elsevier, Amsterdam (1986).

Sivaram, B., and P. K. Swamee, "A Computational Method for Consolidation Coefficient," *J. Japan. Soc. Soil Mech. Found. Eng.*, **17**, 48 (1977).

Taylor, D. W., *Fundamentals of Soil Mechanics*, 5th ed., Wiley, New York, p. 225 (1962).

Terzaghi, K., and P. B. Peck, *Soil Mechanics in Engineering Practice*, Wiley, New York (1948).

Thies-Weesie, D. M. E., and A. P. Phlipse, "Liquid Permeation of Bidisperse Colloidal Hard-sphere Packings and the Kozeny-Carmen Scaling Relation," *J. Colloid Interf. Sci.*, **162**, 470 (1994).

Wakeman, R. J., M. N. Sabri, and E. S. Tarleton, "Factors Affecting the Formation and Properties of Wet Compacts," *Powder Technol.*, **65**, 283 (1991).

Appendix 1: Similarity Solution for Compact Formation

The equations governing filtration in the rheological model are

$$\frac{dP_y}{d\phi}\frac{\partial\phi}{\partial z} = \frac{\lambda}{V_p}\frac{\phi r(\phi)}{(1-\phi)^2}\left(\frac{dh}{dt} + u\right) \qquad (A1)$$

$$\frac{\partial\phi}{\partial t} = \frac{\partial}{\partial z}(\phi u) \qquad (A2)$$

in $0 < z < l(t)$ with boundary conditions

$$P_y[\phi(0,t)] = \Delta p \qquad (A3)$$

$$u(0,t) = 0 \qquad (A4)$$

$$\phi(l,t) = \phi_g \qquad (A5)$$

$$u(l,t)=\left(\frac{\phi_0}{\phi_g}\right)\frac{dh}{dt}+\left(1-\frac{\phi_0}{\phi_g}\right)\frac{dl}{dt}. \tag{A6}$$

In $l(t)<z<h(t)$ we have

$$p_s(z,t)=0 \qquad (\phi_0<\phi_g) \tag{A7}$$

$$p_f(z,t)=\Delta p \tag{A8}$$

$$\phi(z,t)=\phi_0 \tag{A9}$$

$$u(z,t)=-\frac{dh}{dt}. \tag{A10}$$

We introduce the following scaled variables

$$T=t\left\{\frac{k(1-\phi_0)^2}{\phi_0 r(\phi_0)h_0^2}\left(\frac{V_p}{\lambda}\right)\right\} \tag{A11}$$

$$Z=\frac{z}{h_0} \tag{A12}$$

$$H(T)=\frac{h(t)}{h_0} \tag{A13}$$

$$L(T)=\frac{l(t)}{h_0} \tag{A14}$$

$$\Phi(Z,T)=\frac{\phi(z,t)}{\phi_0} \tag{A15}$$

$$U(Z,T)=u(z,t)\left\{\frac{\phi_0 r(\phi_0)h_0}{(1-\phi_0)^2 k}\left(\frac{\lambda}{V_p}\right)\right\} \tag{A16}$$

$$f(\Phi)=\frac{P_y(\phi)}{k} \tag{A17}$$

$$R(\Phi)=\frac{r(\phi)}{(1-\phi)^2}\frac{(1-\phi_0)^2}{r(\phi_0)} \tag{A18}$$

$$D(\Phi)=\frac{\dfrac{df}{d\Phi}}{R(\Phi)} \tag{A19}$$

$$\Sigma=\frac{\Delta p}{k} \tag{A20}$$

where k is any convenient pressure scale. In terms of these quantities the governing equation is

$$\frac{\partial\Phi}{\partial T}=\frac{\partial}{\partial Z}\left(D(\Phi)\frac{\partial\Phi}{\partial Z}-\Phi\frac{dH}{dT}\right) \tag{A21}$$

subject to

$$f[\Phi(0,T)]=\Sigma \tag{A22}$$

$$D[\Phi(0)]\left.\frac{\partial\Phi}{\partial Z}\right|_{(0,T)}=\Phi(0)\frac{dH}{dT} \tag{A23}$$

$$\Phi(L,T)=\frac{\phi_g}{\phi_0} \tag{A24}$$

$$D\left(\frac{\phi_g}{\phi_0}\right)\left.\frac{\partial\Phi}{\partial Z}\right|_{(L,T)}=\left(\frac{\phi_g}{\phi_0}-1\right)\left(\frac{dH}{dT}-\frac{dL}{dT}\right). \tag{A25}$$

We define a similarity variable

$$\xi=\frac{Z}{\sqrt{T}} \tag{A26}$$

and seek a solution to Eq. A21 in the form

$$\Phi(Z,T)=\Phi(\xi) \tag{A27}$$

with

$$H(T)=1-\beta\sqrt{T} \tag{A28}$$

$$L(T)=\gamma\sqrt{T}. \tag{A29}$$

We note that $Z=0$ becomes $\xi=0$ and $Z=L$ becomes $\xi=\gamma$. The constants β, γ are to be found.

Equation A21 becomes

$$\frac{d}{d\xi}\left(D(\Phi)\frac{d\Phi}{d\xi}\right)+\frac{(\xi+\beta)}{2}\frac{d\Phi}{d\xi}=0 \tag{A30}$$

with boundary conditions

$$f[\Phi(0)]=\Sigma \tag{A31}$$

$$D[\Phi(0)]\left.\frac{d\Phi}{d\xi}\right|_0=-\frac{\Phi(0)\beta}{2} \tag{A32}$$

$$\Phi(\gamma)=\frac{\phi_g}{\phi_0} \tag{A33}$$

$$D\left(\frac{\phi_g}{\phi_0}\right)\left.\frac{d\Phi}{d\xi}\right|_\gamma=\left(1-\frac{\phi_g}{\phi_0}\right)\left(\frac{\beta+\gamma}{2}\right). \tag{A34}$$

The method of solution is as follows—guess a value of β and solve Eq. A30 from $\xi=0$ to the point $\xi=\gamma^*$ where

$$\Phi(\gamma^*)=\frac{\phi_g}{\phi_0}. \tag{A35}$$

If

$$D\left(\frac{\phi_g}{\phi_0}\right)\left.\frac{d\Phi}{d\xi}\right|_{\gamma^*}=\left(1-\frac{\phi_g}{\phi_0}\right)\left(\frac{\beta+\gamma^*}{2}\right), \tag{A36}$$

then β is correct and $\gamma=\gamma^*$. If Eq. A36 is not correct, then we adjust β and iterate. Thus β and γ are found as part of the solution of the differential equation.

Appendix 2: Similarity Solution for Consolidation Stage

In scaled variables we require the solution to

$$\frac{\partial \Phi}{\partial T} = \frac{\partial}{\partial Z}\left[D(\Phi)\frac{\partial \Phi}{\partial Z} - \Phi\frac{dH}{dT}\right] \tag{A37}$$

subject to $\Phi(0, T)$ given by virtue of

$$f[\Phi(0)] = \Sigma \tag{A38}$$

$$\frac{\partial \Phi}{\partial Z}(0, T) = \frac{\Phi(0)}{D[\Phi(0)]}\frac{dH}{dT} \tag{A39}$$

$$\frac{\partial \Phi}{\partial Z}(H, T) = 0 \tag{A40}$$

and the normalization condition

$$\int_0^{H(T)} \Phi(Z, T)\, dZ = 1. \tag{A41}$$

In what follows we restart time ($T = 0$) from the beginning of the consolidation stage, and at $T = \infty$ we reach equilibrium where

$$H_\infty = \frac{1}{\Phi(0)}. \tag{A42}$$

Thus

$$H(0) = H_f = \frac{h(t_f)}{h_0}. \tag{A43}$$

We attempt a similarity solution by introducing a similarity variable

$$\xi = \frac{Z}{\sqrt{T}}. \tag{A44}$$

We look for a solution of Eq. A37 in the form

$$\Phi(Z, T) = \Phi(\xi) \tag{A45}$$

with

$$H(T) = H_f - \delta\sqrt{T}. \tag{A46}$$

If this is possible we would therefore have

$$U_c(T) = \frac{H_f - H(T)}{H_f - H_\infty} = S\sqrt{T} \tag{A47}$$

where

$$S = \frac{\delta}{H_f - H_\infty}. \tag{A48}$$

The differential equation (Eq. A37) reduces to

$$\frac{d}{d\xi}\left[D(\Phi)\frac{d\Phi}{d\xi}\right] + \frac{(\xi + \delta)}{2}\frac{d\Phi}{d\xi} = 0 \tag{A49}$$

subject to

$$\left.\frac{d\Phi}{d\xi}\right|_{\xi = 0} = -\frac{\delta}{2}\frac{\Phi(0)}{D[\Phi(0)]} \tag{A50}$$

and

$$\left.\frac{d\Phi}{d\xi}\right|_{\xi = H/\sqrt{T}} = 0 \tag{A51}$$

with $\Phi(0)$ given. We see immediately that a similarity solution is not strictly possible since the boundary condition (Eq. A51) is not independent of the time variable. We note that the conservation condition (Eq. A41) reduces to

$$\int_0^{H/\sqrt{T}} \left(\Phi - \frac{1}{H_f}\right) d\xi = \frac{\delta}{H_f}, \tag{A52}$$

which is again not independent of time.

However, for $T \ll H_f^2$ we have that the upper limit for ξ is $\gg 1$, which implies that a similarity solution can be a good initial approximation for small T. Then the solution of Eq. A49 subject to Eq. A50 and

$$\left.\frac{d\Phi}{d\xi}\right|_{\xi = \infty} = 0 \tag{A53}$$

$$\int_0^{\infty} \left(\Phi - \frac{1}{H_f}\right) d\xi = \frac{\delta}{H_f} \tag{A54}$$

may be an accurate solution for much of the consolidation stage.

We find the value of δ is this approximate similarity solution by iteration. An estimate of δ is chosen and Eq. A49 is solved from $\xi = 0$ where Eq. A50 holds and $\Phi = \Phi(0)$ is given to $\xi = \infty$ where Eq. A53 holds. If δ were correct, then Eq. A54 will be satisfied. If not, δ is adjusted and the solution process recycled. It is possible to show that a value of δ can always be found by this process.

Manuscript received May 2, 1994, and revision received Sept. 6, 1994.